Inorganic Chemistry

Article

pubs.acs.org/IC

Mn_4 Single-Molecule-Magnet-Based Polymers of a One-Dimensional Helical Chain and a Three-Dimensional Network: Syntheses, Crystal Structures, and Magnetic Properties

Hui-Lien Tsai,*[,†] Chen-I Yang,*[,‡] Wolfgang Wernsdorfer,[§] Siang-Hua Huang,[†] Siang-Yu Jhan,[†] Ming-Hsuan Liu,[†] and Gene-Hsiang Lee[∥]

[†]Department of Chemistry, National Cheng Kung University, Tainan 701, Taiwan

[‡]Department of Chemistry, Tunghai University, Taichung 407, Taiwan

[§]Nanosciences Department, Institut Néel, CNRS, BP 166, 25 Avenue des Martyrs, 38042 Grenoble Cedex 9, France

[∥]Instrumentation Center, College of Science, National Taiwan University, Taipei 106, Taiwan

Supporting Information

ABSTRACT: Two Mn_4 single-molecule-magnet (SMM)-based coordination polymers, $\{[Mn_4O(salox)_3(N_3)_3(DMF)_2(H_2O)(dpp)]\cdot 0.5MeOH\}_n$ (**1**·0.5MeOH; H_2salox = salicylaldoxime; dpp = 1,3-di-4-pyridylpropane; DMF = *N*, *N*-dimethylformamide) and $\{[Mn_4O(Me\text{-}salox)_3(N_3)_3(dpp)_{1.5}]\cdot 1.5Et_2O\}_n$ (**2**·1.5Et_2O; Me-H_2salox = hydroxyphenylethanone oxime), are self-assembled from $Mn(ClO_4)_2\cdot 6H_2O$/H_2salox and $Mn(ClO_4)_2\cdot 6H_2O$/Me-H_2salox systems with dpp and NaN_3 in DMF/MeOH, respectively. Both compounds comprise a mixed-valence tetranuclear manganese core, $[Mn^{II}Mn^{III}_3O]^{9+}$, which serves as a building unit for subsequent assembly via oximate and azido ligands. The flexible dpp ligand links with a Mn_4 unit, leading to the formation of a one-dimensional helical structure in **1**·0.5MeOH and a three-dimensional *pcu* network in **2**·1.5Et_2O. The magnetic data analysis shows that antiferromagnetic interactions within the Mn_4 units resulted in $S = {}^3/_2$ and ${}^7/_2$ ground states for **1**·0.5MeOH and **2**·1.5Et_2O, respectively. Both compounds show SMM behavior, as evidenced by frequency-dependent out-of-phase signals in alternating-current magnetic susceptibility and magnetic hysteresis loop studies with an energy barrier of U_{eff} = 37 K for **2**·1.5Et_2O.

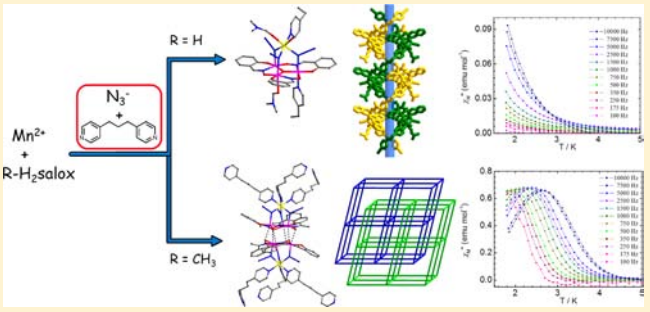

INTRODUCTION

Polynuclear manganese clusters have received considerable interest in recent years. Considerable effort has been devoted to understanding the structures and properties of the synthetic models for mimicking the active site of metalloenzymes that contain oxide-bridged manganese cores, such as the water-oxidizing complex of photosystem II[1] and catalase enzymes.[2] Manganese clusters often exhibit large, and sometimes abnormally large, spin values in the ground state, and combined with a large anisotropy, some of these species are single-molecule magnets (SMMs) or single-chain magnets (SCMs). SMMs show a significant barrier to magnetization relaxation arising from the combination of a large ground-state spin, *S*, with an easy-axis anisotropy (negative zero-field-splitting parameter, *D*).[3−6] SCMs exhibit a large uniaxial anisotropy and strong intrachain exchange interactions without spin compensation between the high-spin magnetic units, with good isolation of the chains that prevents two- (2D) and three-dimensional (3D) ordering.[7−9] An important future development for SMMs and SCMs is the discovery of synthetic schemes that can yield new compounds and families of related compounds with large spins and/or significant magnetoanisotropies.[10] It is known that the Mn^{III}-ion Jahn−Teller (JT) elongation plays an importance role in SMM and SCM properties and that the orientations of JT elongation significantly affect the energy barrier.[11] Thus, many current routes for producing SMMs and SCMs involve Mn^{III}-containing compounds to exploit the associated large single-ion anisotropy.[9a,b,10]

More recently, the use of manganese clusters as building blocks for the construction of coordination polymers as one-dimensional (1D),[12] 2D,[13] and, in very few examples, 3D[14] structures with interesting magnetic properties was also investigated. Theoretically, such an arrangement of molecular magnets in a crystalline material would enable magnetization probing without the interference of magnetic ordering, allowing researchers to study the exact nature of the retention of magnetization for SMMs.[14a,15] A synthetic methodology that has proven to be successful in the synthesis of such compounds is the reaction of linking ligands with chelating coligands, which

Received: July 3, 2012
Published: December 6, 2012

   dx.doi.org/10.1021/ic3014333 | *Inorg. Chem.* 2012, 51, 13171−13180

may subserve the formation of manganese clusters. Salicylaldoxime-containing manganese compounds are considered to be good candidates as building units for these materials because they usually comprise a $[Mn_3O]^{7+}$ triangle core, which is magnetically interesting because of the pronounced magnetic anisotropy from its almost near-parallel JT distortion axes in high-spin Mn^{III} ions. Some of these compounds have been reported as SMMs[16] and as building blocks of a 1D chain.[17]

Using salicylaldoxime and its derivatives (H_2salox and Me-H_2salox) with azido ligands and 1,3-di-4-pyridylpropane (dpp) is attractive for the above applications. The combination of salicylaldoxime and azido ligands is known in cluster coordination chemistry especially for SMMs,[18] but it has few uses in coordination polymers.[17a,19] The present study used these ligands to prepare two new compounds, $\{[Mn_4O(salox)_3(N_3)_3(DMF)_2(H_2O)(dpp)]\cdot 0.5MeOH\}_n$ (**1**·0.5MeOH; H_2salox = salicylaldoxime; dpp = 1,3-di-4-pyridylpropane; DMF = *N*,*N*-dimethylformamide) and $\{[Mn_4O(Me\text{-}salox)_3(N_3)_3(dpp)_{1.5}]\cdot 1.5Et_2O\}_n$ (**2**·1.5Et_2O; Me-H_2salox = hydroxyphenylethanone oxime). The former adopts an 1D helical structure, and the latter shows a 3D *pcu* network. Both compounds are constructed from an unprecedented Mn_4 topology building unit. These two compounds not only show interesting topologies but also exhibit SMM behaviors resulting from the significant magnetic anisotropy of the Mn_4 unit. The detailed syntheses, structures, and magnetic properties of these compounds are described below.

EXPERIMENTAL SECTION

Synthesis. All solvents and reagents where used as-received; no purification was necessary. All reactions were performed under aerobic conditions. ***Caution!*** *Perchlorate compounds are potentially explosive; such compounds should be synthesized, used in small quantities, and treated with the utmost care at all times. The derived oximes were prepared via a condensation reaction, as previously reported.*[20]

*$\{[Mn_4O(salox)_3(N_3)_3(DMF)_2(H_2O)(dpp)]\cdot 0.5MeOH\}_n$ (**1**·0.5MeOH).* $Mn(ClO_4)_2\cdot 6H_2O$ (181 mg, 0.50 mmol) and NaN_3 (64.5 mg, 0.99 mmol) were dissolved in a 1:1 MeOH/DMF mixture (20 mL). To this was added H_2salox (68.3 mg, 0.50 mmol) and NEt_3 (50.4 mg, 0.50 mmol), resulting in a deep-green solution. After stirring for 5 min, dpp (100.1 mg, 0.50 mmol) was added, followed by stirring for 30 min, during which time the solution turned dark green. The vapor diffusion of Et_2O into the solution slowly produced crystals. After 1 week, well-formed deep-green crystals appeared. The sample for crystallographic study, identified as **1**·0.5MeOH, was maintained in contact with the mother liquor to avoid solvent loss. The yield was 60% (based on Mn). Anal. Calcd (found) for $C_{40.5}H_{47}Mn_4N_{16}O_{10.5}$ (**1**·0.5MeOH): C, 47.46 (47.18); H, 4.13 (4.12); N, 19.56 (19.63). IR data (KBr disk, cm^{-1}): 3422 (br, s), 2928 (m), 2075 (vs), 2059 (vs), 1655 (s), 1596 (s), 1541 (m), 1439 (s), 1386 (w), 1327 (m), 1284 (s), 1202 (m), 1152 (w), 1122 (w), 1107 (w), 1042 (s), 1068 (s), 918 (s), 819 (w), 760 (s), 679 (vs), 647 (s), 465 (m).

*$\{[Mn_4O(Me\text{-}salox)_3(N_3)_3(dpp)_{1.5}]\cdot 1.5Et_2O\}_n$ (**2**·1.5Et_2O).* The procedure was the same as that employed for compound **1**, except that an excess of Me-H_2salox (75.5 mg, 0.50 mmol) was added instead of H_2salox. Deep-green crystals were obtained. The yield was 68% (based on Mn). The sample used for crystallography, identified as **2**·1.5Et_2O, was maintained in contact with the mother liquor to avoid solvent loss. Dried solid was hygroscopic and analyzed as **2**·2H_2O. Anal. Calcd (found) for $C_{43.5}H_{36}Mn_4N_{16}O_{11}$ (**2**·2H_2O): C, 45.72 (46.27); H, 4.06 (4.68); N, 18.39 (18.07). Selected IR data (KBr disk, cm^{-1}): 3433 (br, s), 2930 (m), 2057 (vs), 1653 (s), 1612 (s), 1595 (s), 1569 (m), 1527 (m), 1473 (w), 1434 (s), 1384 (w), 1315 (s), 1281 (w), 1247 (m), 1134 (w), 1052 (m), 1021 (m), 971 (s), 864 (m), 806 (w), 759 (m), 678 (vs), 650 (m), 607 (m), 571 (m), 545 (w), 519 (w), 477 (w), 438 (m).

X-ray Crystallography. The single crystals of **1**·0.5MeOH and **2**·1.5Et_2O were mounted on the tip of a glass fiber with dimensions of 0.50 × 0.35 × 0.03 and 0.22 × 0.20 × 0.20 mm^3, respectively. Intensity data were collected at 150(2) K within the limits of 1.49° < θ < 27.50° for **1**·0.5MeOH and 1.44° < θ < 27.50° for **2**·1.5Et_2O using a Nonius Kappa CCD diffractometer equipped with graphite-monochromatized Mo Kα radiation (λ = 0.71073 Å). The structures were solved by direct methods and refined by the full-matrix least-squares method on F^2 values using the *SHELX-97*[21] program package. All non-hydrogen atoms were refined anisotropically, whereas the hydrogen atoms were placed in ideal, calculated positions, with isotropic thermal parameters riding on their respective carbon atoms. In **1**·0.5MeOH, one of the coordinated DMF molecules is disordered over two positions with site occupation factors (SOFs) of 0.55 and 0.45, and the solvated MeOH is disordered with a SOF of 0.5. In **2**·1.5Et_2O, Et_2O is disordered over two positions with a SOF of 0.5. The experimental details for X-ray data collection and refinements of **1**·0.5MeOH and **2**·1.5Et_2O are presented in Table 1.

Table 1. Crystallographic Data for 1·0.5MeOH and 2·1.5Et_2O

	1·0.5MeOH	**2**·1.5Et_2O
formula	$C_{40.5}H_{47}Mn_4N_{16}O_{10.5}$	$C_{49.5}H_{57}Mn_4N_{15}O_{8.5}$
M_w	1145.70	1217.86
cryst syst	monoclinic	rhombohedral
space group	*C*2/*c*	$R\bar{3}c$
a/Å	27.6680(14)	19.3717(7)
b/Å	12.5270(6)	19.3717(7)
c/Å	29.3747(16)	52.616(2)
α/deg	90	90
β/deg	111.282(2)	90
γ/deg	90	120
V/Å^3	9486.9(8)	17099.5(11)
Z	8	12
λ/Å	0.71073	0.71073
T/K	150(2)	150(2)
D_c/g cm^{-3}	1.640	1.419
μ/mm^{-1}	1.116	0.930
$\Delta\rho_{max}$, $\Delta\rho_{min}$/e Å^{-3}	0.171, 0.917	0.248, 0.978
measd/indep reflns (R_{int})	22148/10764 (0.0527)	29916/4350 (0.0833)
obsd reflns [$I > 2\sigma(I)$]	7302	3176
GOF on F^2	1.013	1.065
R1,[a] wR2[b] (all data)	0.0557, 0.1360	0.0638, 0.1845
R1,[a] wR2[b] [$I > 2\sigma(I)$]	0.0927, 0.1620	0.0964, 0.2109

[a] $R1 = (\sum||F_o| - |F_c||)/\sum|F_o|$. [b] $wR2 = [\sum[w(F_o^2 - F_c^2)^2]/\sum[w(F_o^2)^2]]^{1/2}$.

Physical Measurements. IR spectra were recorded for the solid state (KBr pellets) on a Nicolet Magna 550 Fourier transform IR spectrometer in the range of 4000−400 cm^{-1}. Elemental analyses were carried out using an Elementar Vario EL III analyzer. Thermogravimetric analyses (TGA) were performed under nitrogen with a Shimadzu TGA-50 analyzer. Powder X-ray diffraction (PXRD) data were recorded on a Shimadzu XRD-7000S X-ray diffractometer at 30 kV and 30 mA with Cu Kα radiation (λ = 1.5406 Å), with a step size of 0.028 in θ and a scan speed of 1 s $step^{-1}$. Variable-temperature direct-current (dc) and alternating-current (ac) magnetic susceptibility measurements were collected on microcrystalline samples, restrained in eicosane to prevent torquing, on a Quantum Design MPMS-XL SQUID and a PPMS magnetometer equipped with 7.0 and 9.0 T magnets, respectively, operated in the range of 1.8−300.0 K. Diamagnetic corrections were estimated from Pascal's constants[22] and subtracted from the experimental susceptibility data to obtain the molar paramagnetic susceptibilities of the compounds.

RESULTS AND DISCUSSION

Synthesis. The salicylaldoxime group (H_2salox) has been used as a chelating ligand in metal cluster chemistry.[23] It has been observed in its singly deprotonated ($Hsalox^-$) form as a

dx.doi.org/10.1021/ic3014333 | *Inorg. Chem.* 2012, 51, 13171−13180

Table 2. Selected Bond Distances (Å) and Angles (deg) for Compounds 1·0.5MeOH and 2·1.5Et_2O

1·0.5MeOH			
Mn1−O1	1.885(3)	Mn2−Mn3	3.2337(9)
Mn1−O2	1.894(3)	Mn3−O6	1.862(3)
Mn1−O5	1.919(3)	Mn3−O1	1.870(3)
Mn1−N1	2.018(3)	Mn3−O3	1.910(3)
Mn1−N4	2.308(3)	Mn3−N3	2.002(3)
Mn1−N14#1	2.355(3)	Mn3−N10	2.136(4)
Mn2−O4	1.856(3)	Mn4−O9	2.165(3)
Mn2−O1	1.887(3)	Mn4−N7	2.205(4)
Mn2−O7	1.904(3)	Mn4−N4	2.228(3)
Mn2−N2	2.001(3)	Mn4−N10	2.234(3)
Mn2−N7	2.296(4)	Mn4−O8	2.262(3)
Mn2−O10	2.451(4)	Mn4−N13	2.276(4)
O1−Mn1−O2	178.50(12)	N2−Mn2−Mn3	120.49(9)
O1−Mn1−O5	92.67(11)	N7−Mn2−Mn3	86.91(9)
O2−Mn1−O5	87.62(12)	O10−Mn2−Mn3	94.42(9)
O1−Mn1−N1	88.84(12)	O6−Mn3−O1	165.83(12)
O2−Mn1−N1	90.92(12)	O6−Mn3−O3	85.74(11)
O5−Mn1−N1	177.26(12)	O1−Mn3−O3	91.89(11)
O1−Mn1−N4	87.72(11)	O6−Mn3−N3	89.65(13)
O2−Mn1−N4	90.79(12)	O1−Mn3−N3	89.31(13)
O5−Mn1−N4	95.10(12)	O3−Mn3−N3	165.83(14)
N1−Mn1−N4	87.24(12)	O6−Mn3−N10	95.60(13)
O1−Mn1−N14#1	93.00(12)	O1−Mn3−N10	98.56(12)
O2−Mn1−N14#1	88.45(12)	O3−Mn3−N10	99.15(13)
O5−Mn1−N14#1	92.77(12)	N3−Mn3−N10	94.62(15)
N1−Mn1−N14#1	84.87(12)	O6−Mn3−Mn2	149.59(9)
N4−Mn1−N14#1	172.06(12)	O1−Mn3−Mn2	30.76(8)
O4−Mn2−O1	177.69(13)	O3−Mn3−Mn2	122.58(8)
O4−Mn2−O7	86.75(13)	N3−Mn3−Mn2	60.16(10)
O1−Mn2−O7	91.63(12)	N10−Mn3−Mn2	90.75(10)
O4−Mn2−N2	91.02(13)	O9−Mn4−N7	91.16(14)
O1−Mn2−N2	90.22(12)	O9−Mn4−N4	171.00(14)
O7−Mn2−N2	167.59(16)	N7−Mn4−N4	87.04(13)
O4−Mn2−N7	89.77(15)	O9−Mn4−N10	90.57(13)
O1−Mn2−N7	92.09(12)	N7−Mn4−N10	90.45(13)
O7−Mn2−N7	98.61(15)	N4−Mn4−N10	98.26(12)
N2−Mn2−N7	93.58(13)	O9−Mn4−O8	81.24(12)
O4−Mn2−O10	91.59(15)	N7−Mn4−O8	97.80(12)
O1−Mn2−O10	86.67(12)	N4−Mn4−O8	90.26(11)
O7−Mn2−O10	86.29(16)	N10−Mn4−O8	168.45(12)
N2−Mn2−O10	81.57(14)	O9−Mn4−N13	93.49(14)
N7−Mn2−O10	174.98(14)	N7−Mn4−N13	173.58(13)
O4−Mn2−Mn3	148.46(10)	N4−Mn4−N13	89.03(12)
O1−Mn2−Mn3	30.45(8)	N10−Mn4−N13	85.08(13)
O7−Mn2−Mn3	62.85(9)	O8−Mn4−N13	87.29(12)

2·1.5Et_2O			
Mn1−N1	2.243(4)	Mn2−O2#1	1.867(3)
Mn1−N1#1	2.243(4)	Mn2−O1	1.8842(7)
Mn1−N1#2	2.243(4)	Mn2−O3	1.934(3)
Mn1−N5#1	2.292(4)	Mn2−N4#1	1.992(4)
Mn1−N5	2.292(4)	Mn2−N1	2.182(4)
Mn1−N5#2	2.292(4)		
N1−Mn1−N1#1	91.65(13)	N5#1−Mn1−N5#2	93.01(13)
N1−Mn1−N1#2	91.65(13)	N5−Mn1−N5#2	93.01(13)
N1#1−Mn1−N1#2	91.65(13)	O2#1−Mn2−O1	177.33(14)
N1−Mn1−N5#1	90.17(13)	O2#1−Mn2−O3	93.93(13)
N1#1−Mn1−N5#1	85.27(13)	O1−Mn2−O3	87.77(11)
N1#2−Mn1−N5#1	176.47(14)	O2#1−Mn2−N4#1	89.46(14)
N1−Mn1−N5	85.27(13)	O(1)−Mn(2)−N(4)#1	88.22(10)
N1#1−Mn1−N5	176.47(14)	O3−Mn2−N4#1	158.81(14)
N1#2−Mn1−N5	90.17(14)	O2#1−Mn2−N1	90.57(14)
N5#1−Mn1−N5	93.01(13)	O1−Mn2−N1	91.33(18)
N1−Mn1−N5#2	176.47(14)	O3−Mn2−N1	95.35(14)
N1#1−Mn1−N5#2	90.17(14)	N4#1−Mn2−N1	105.54(14)
N1#2−Mn1−N5#2	85.27(13)		

bidentate chelate with the protonated N−OH not bound,[24] but it more commonly occurs in its doubly deprotonated ($salox^{2-}$) form as a tridentate chelate.[25] The variety of binding modes of H_2salox may allow the synthesis of new nuclearities and topologies. The treatment of a MeOH/DMF mixture solution of $Mn(ClO_4)_2·6H_2O$, NEt_3, NaN_3, H_2salox, and dpp in a 1:1:1:1:1 ratio led to a dark-green reaction mixture. The residue was slowly diffused with Et_2O to yield dark-green-brown triangular crystals of **1**·0.5MeOH in 60% yield. When the reaction process of compound **1** was carried out with equivalent Me-H_2salox instead of H_2salox, compound **2**·1.5Et_2O was obtained in a yield of 68%. The reactions of compounds **1** and **2** are summarized in eqs 1 and 2, respectively.

$$16Mn(ClO_4)_2·6H_2O + 12H_2salox + 12NaN_3 + 8DMF + 4dpp + 2MeOH + 3O_2 \rightarrow 4\mathbf{1}·0.5MeOH + 32ClO_4^- + 94H_2O + 20H^+ + 12Na^+ \quad (1)$$

$$16Mn(ClO_4)_2·6H_2O + 12Me\text{-}H_2salox + 12NaN_3 + 6dpp + 6Et_2O + 3O_2 \rightarrow 4\{[Mn_4O(Me\text{-}salox)_3(N_3)_3(dpp)_{1.5}]·1.5Et_2O\}_n + 32ClO_4^- + 94H_2O + 20H^+ + 12Na^+ \quad (2)$$

These reactions involve manganese oxidation, undoubtedly by O_2 under the prevailing basic conditions, and have been balanced accordingly. NEt_3 ensures basic conditions and acts as a proton acceptor; in its absence, longer reaction times (>24 h) are required to get a significant dark-red coloration, and the yields of isolated **1**·0.5MeOH and **2**·1.5Et_2O are much lower (<5%). On the other hand, >2 equiv of NEt_3 gave insoluble amorphous precipitates that were probably manganese oxides or oxo/hydroxides. An increase in the amount of H_2salox or Me-H_2salox to 3 equiv (or more) led to the isolation of **1**·0.5MeOH and **2**·1.5Et_2O in low yields of <10%.

Description of the Crystal Structures. Single crystals of compounds **1**·0.5MeOH and **2**·1.5Et_2O suitable for single-crystal X-ray crystallography were obtained. Labeled plots of crystal structures and packing diagrams for both compounds are shown in Figures 1−5. The selected bond distances and angles are listed in Table 2.

1·0.5MeOH. X-ray structural analysis shows that **1**·0.5MeOH crystallized in monoclinic space group *C*2/*c* and that the asymmetric unit contains the whole Mn_4 unit and half of MeOH. As shown in Figure 1, compound **1**·0.5MeOH has a covalently bonded 1D structure, which was built from Mn_4 clusters connected by one dpp ligand. The **1**·0.5MeOH molecule does not have any crystallographic symmetry. Bond-valence-sum (BVS)[26] calculations (Table 3) and close examination of the structural parameters agree with a valence-trapped description of

dx.doi.org/10.1021/ic3014333 | Inorg. Chem. 2012, 51, 13171−13180

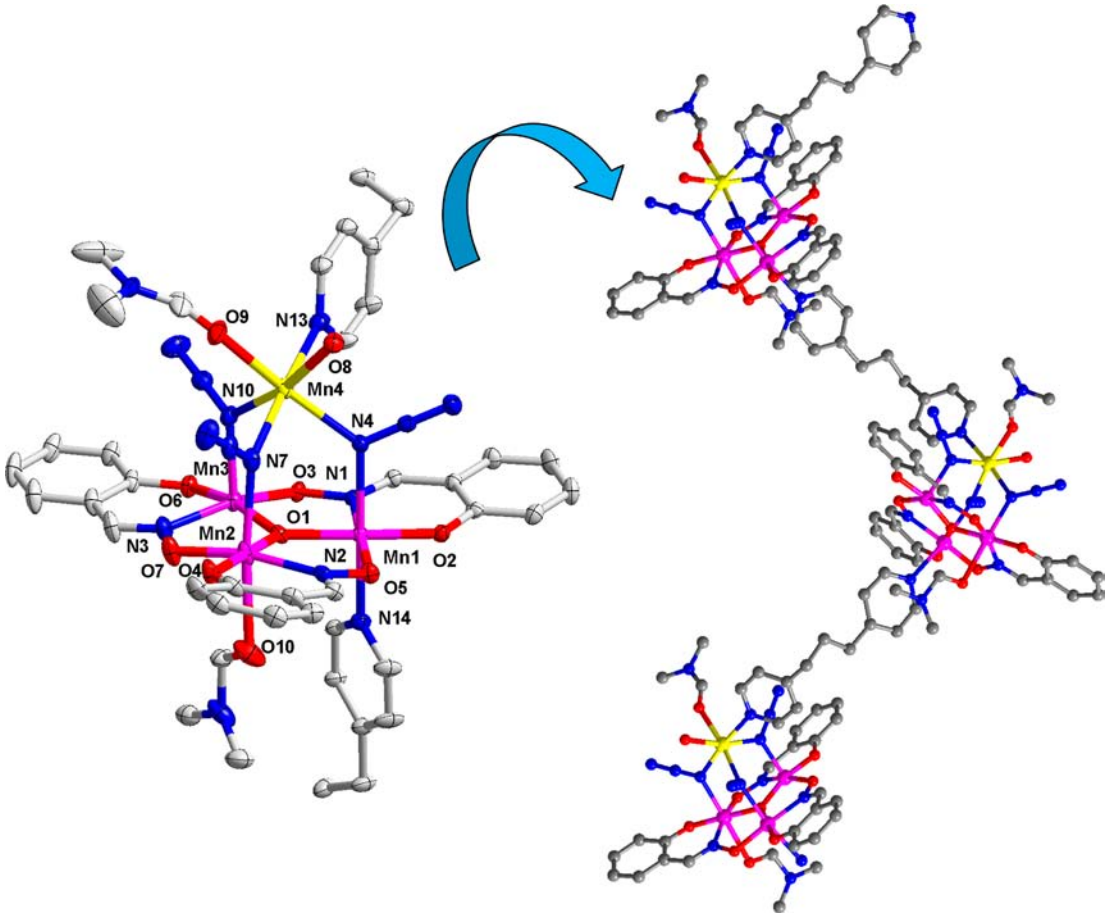

Figure 1. ORTEP drawing of the asymmetric unit of **1**·0.5MeOH with thermal ellipsoids set at 30% probability. Hydrogen atoms and solvated molecules have been omitted for clarity (right). The 1D chain structure of **1**·0.5MeOH is viewed along the *a* axis.

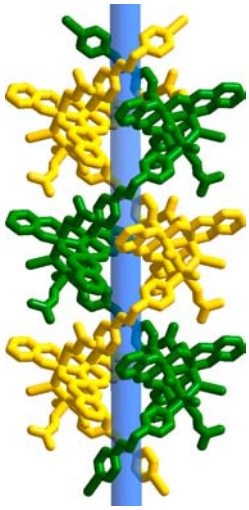

Figure 2. Structure of a double-helical chain assembly of **1**.

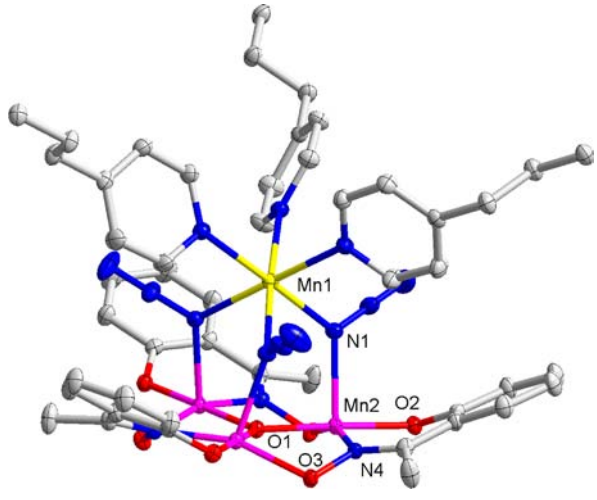

Figure 3. ORTEP drawing of a Mn_4 cluster in **2**·1.5Et_2O. Hydrogen atoms and solvated molecules have been omitted for clarity.

Mn1−Mn3 being Mn^{III} and Mn4 being Mn^{II}. The Mn^{III} centers of Mn1 and Mn2 are six-coordinated, each of them clearly possessing a JT distortion in the form of axis elongation along N1−Mn1−N14 and N7−Mn2−O10, whereas Mn3 adopts a five-coordinated geometry, which is regarded as a square pyramid (τ < 0.001), in which the nitrogen atom of an end-on azide is located in the apical position.[27] As expected, the JT axes are located so as to avoid Mn−O^{2-} bonds, which are the shortest and strongest in the molecule (<1.9 Å), and the JT axes at the two Mn^{III} ions in the compound are nearly parallel. The structure of the Mn_4 cluster can be described as a distorted triangular pyramid, whose basal plane is constructed by a μ-O^{2-}, which lies ∼0.118 Å below the plane of the three manganese ions and whose centered [Mn^{III}_3O] triangle and apical is occupied by a Mn^{II} ion. Each Mn^{III} ion of the triangle is bridged to the apical Mn^{II} by three end-on azido ligands. Each edge of the triangle is bridged by

dx.doi.org/10.1021/ic3014333 | *Inorg. Chem.* 2012, 51, 13171−13180

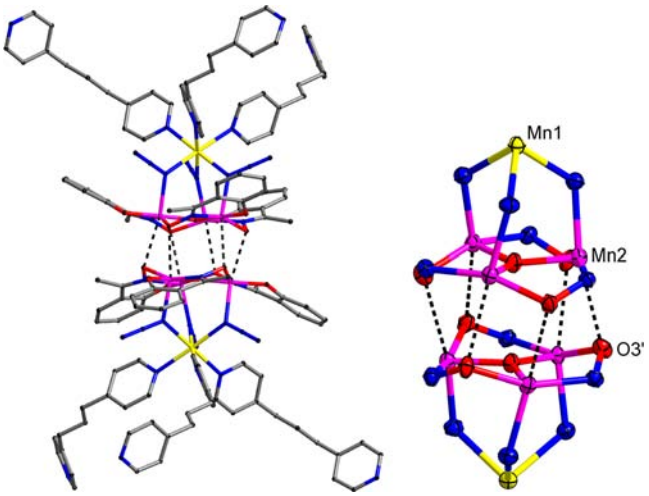

Figure 4. Structure drawing of the $(Mn_4)_2$ unit in **2**.

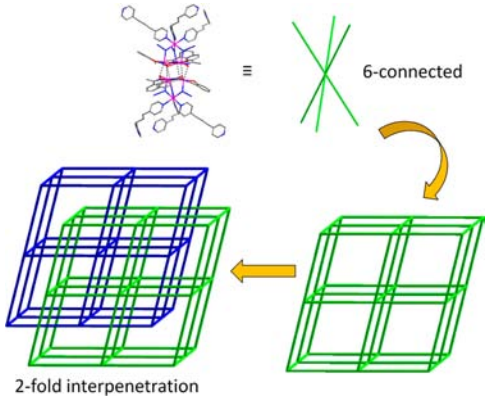

Figure 5. Schematic representation of a 3D *pcu* framework in **2**, including chemical structures of the components.

Table 3. BVS Calculation Results of Manganese Centers for Compounds 1·0.5MeOH and 2·1.5Et$_2$O

	Mn1	Mn2	Mn3	Mn4
	Compound **1**·0.5MeOH			
Mn^{II}	3.24	3.33	3.31	***1.84***
Mn^{III}	***2.99***	***3.07***	***3.05***	1.70
Mn^{IV}	2.93	3.01	2.99	1.67
	Compound **2**·1.5Et$_2$O			
Mn^{II}	***1.65***	3.19		
Mn^{III}	1.53	***2.94***		
Mn^{IV}	1.5	2.89		

a dianionic oximate group of a salox^{2-} ligand in the $\eta^1{:}\eta^1{:}\eta^1{:}\mu_2$ mode, whose each deprotonated hydroxyl group is bound terminally to a Mn^{III} ion to form a Mn−O−N−Mn chelating ring. The chelating rings are slightly distorted from planarity with torsion angles of 14.81°, 0.57°, and 15.60° for Mn1−O5−N2−Mn2, Mn2−O7−N3−Mn3, and Mn3−O3−N1−Mn1, respectively. The peripheral ligations in the Mn_4 unit are provided by one water molecule, two DMF molecules, and one dpp ligand. The flexible dpp ligand adapts a trans−gauche conformation and connects to Mn1′ in the neighboring Mn_4 unit, forming a 1D helical structure (Figure 2) along the *b* axis. Moreover, the adjacent left- and right-handed helical chains are cross-linked into a double-helical chain structure by the hydrogen bonding of solvated MeOH.

2·1.5Et$_2$O. Single-crystal X-ray diffraction analysis reveals that compound **2**·1.5Et$_2$O crystallizes in rhombohedral space group $R\bar{3}c$. Similar to compound **1**, the compound contains a mixed-valence $Mn^{II}Mn^{III}_3$ cluster (Figure 3), the structural geometry of each Mn_4 cluster in which the oxidation state of each metal center is evidenced by BVS (Table 3) and JT elongation axes. The Mn_4 cluster adopts a distorted trigonal-pyramidal geometry with a basal plane of a $[Mn^{III}_3O]$ triangle and an apex occupied a Mn^{II} ion. The Mn^{II} ion of Mn1 is six-coordinated with a distorted octahedral geometry, and the Mn^{III} center of Mn2 adopts a five-coordinated geometry, which is regarded as a distorted square pyramid (τ = 0.31), in which the nitrogen atom of the end-on azide is located in the apical position. The Me-salox^{2-} ligand bridges the edge of the $[Mn^{III}_3O]$ triangle with a resulting Mn2−O3−N4−Mn2′ torsion angle of 43.13°. In compound **2**·1.5Et$_2$O, two Mn_4 clusters are connected in the face-to-face arrangement of their $[Mn^{III}_3O]$ to form a $(Mn_4)_2$ subunit through the weak interaction of Mn2···O3′ with a distance of 2.736 Å (Figure 4). The $(Mn_4)_2$ subunits are further linked by three dpp ligands (Mn1−Mn1′) in a trans−trans conformation, forming a 3D framework. If the $(Mn_4)_2$ units linked by three dpp groups are viewed as one node, compound **2**·1.5Et$_2$O can be considered as a six-connected *pcu* topology structure with a 2-fold interpenetrating 3D architecture with another independent equivalent framework (Figure 5).

TGA and PXRD. The thermal stabilities of **1**·0.5MeOH and **2**·1.5Et$_2$O were examined. The results of TGA are in good agreement with the crystallographic observations. A TGA trace of **1** shows that water removal continues in several steps, resulting in a total weight loss of 15.4% in the temperature range of 30−200 °C, corresponding to the loss of a guest MeOH molecule, two coordinated DMF molecules, and one water molecule (calcd, 15.8%). Compound **2** is stable up to 150 °C. Decomposition of **1** and **2** started at 200 and 150 °C, respectively (Figure S1 in the Supporting Information).

PXRD patterns were obtained for compounds **1**·0.5MeOH and **2**·1.5Et$_2$O. The PXRD patterns of the two compounds are in good agreement with the patterns simulated from the respective single-crystal data, confirming the bulk purity of the two samples (Figures S2 and S3 in the Supporting Information).

Magnetic Properties. Solid-state, variable-temperature magnetic susceptibility measurements were performed on microcrystalline samples of compounds **1**·0.5MeOH and **2**·2H$_2$O, all suspended in eicosane to prevent torquing. The dc magnetic susceptibility data of compounds **1**·0.5MeOH and **2**·2H$_2$O were collected in the 2.0−300 K range in a 1.0 kG magnetic field and are illustrated in Figures 6a and 7a, respectively. The value of $\chi_M T$ for **1**·0.5MeOH steadily decreases from 11.4 emu K mol^{-1} at 300 K to 5.8 emu K mol^{-1} at 14 K, below which the $\chi_M T$ value decreases rapidly to 3.4 emu mol^{-1} K at 1.8 K. The values at 300 K are slightly less than the calculated spin-only value of 13.4 emu K mol^{-1} for a $Mn^{II}Mn^{III}_3$ compound with non-interacting metal centers with g = 2.0, suggesting antiferromagnetic interactions. The monotonically decreasing $\chi_M T$ with temperature and the resultant low value of $\chi_M T$ at 2.0 K are indicative of a small ground state for compound **1**·0.5MeOH. In order to characterize the coupling interactions between manganese centers within the Mn_4 unit of **1**·0.5MeOH, the magnetic susceptibility data were fit to the appropriate theoretical expression. Considering the topologies and symmetry of the Mn_4 cluster, a three-*J* model was introduced (Figure 6b). In the model, couplings are characterized as Mn^{III}−Mn^{III} through μ_3-O^{2-} and oximate bridgings (Mn1−Mn2 and Mn1−Mn3 for J_1

dx.doi.org/10.1021/ic3014333 | *Inorg. Chem.* 2012, 51, 13171−13180

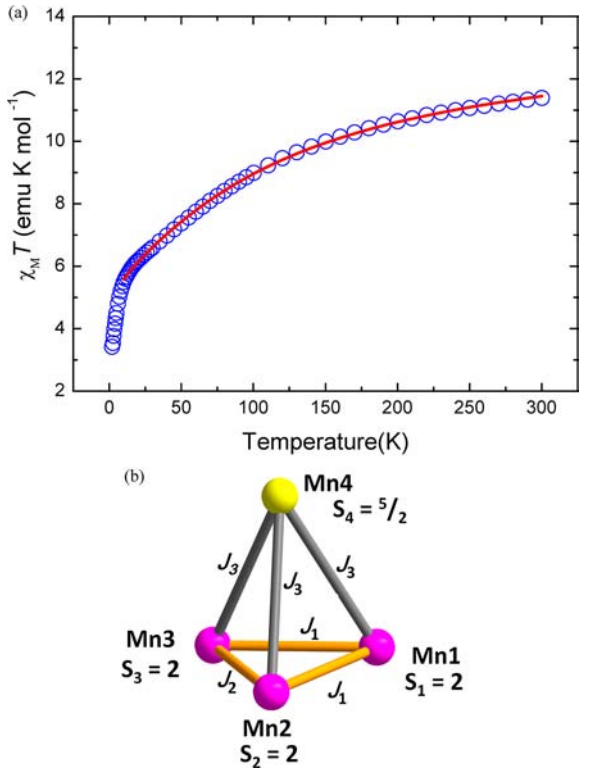

Figure 6. (a) Plot of $\chi_M T$ versus T for microcrystalline samples of compound **1**·0.5MeOH. The solid lines represent a least-squares fit of the data in the region 10−300 K to the van Vleck equation. (b) Diagram showing the definitions of the atom number and magnetic exchange parameters for compound **1**·0.5MeOH.

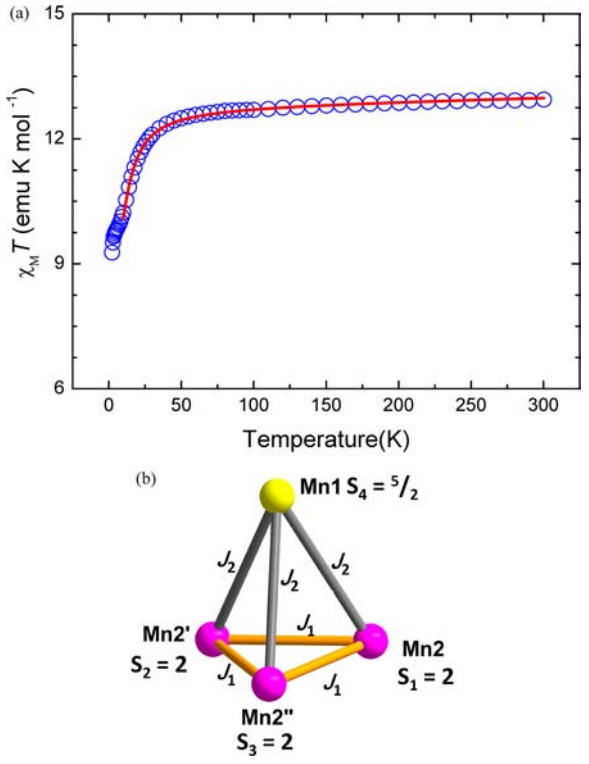

Figure 7. Plot of $\chi_M T$ versus T for microcrystalline samples of compound **2**·2H$_2$O. The solid lines represent a least-squares fit of the data in the region 10−300 K to the van Vleck equation. (b) Diagram showing the definitions of the atom number and magnetic exchange parameters for compound **2**·2H$_2$O.

and Mn2−Mn3 for J_2 based on the torsion angle) and Mn^{II}−Mn^{III} through $\mu_{1,1}$-N_3^- bridging (Mn1−Mn4, Mn2−Mn4, and Mn3−Mn4 for J_3). The spin Hamiltonian that describes the isotropic magnetic exchange interaction is given as

$$H = -2J_2(S_2S_3) - 2J_1(S_1S_2 + S_1S_3) - 2J_3(S_1S_4 + S_2S_4 + S_3S_4) \quad (3)$$

For a compound with three $S = 2$ and one $S = {}^5/_2$ interacting ions, the overall degeneracy of this spin system is 95, which make up a total of 9 possible states with S_T, the total spin of a Mn^{II}Mn$^{III}_3$ cluster, ranging from 0 to ${}^{17}/_2$. A theoretical expression for the molar paramagnetic susceptibility (χ_M) versus temperature (T) was derived using the van Vleck equation and assuming an isotropic g value. This expression was used to fit the experimental χ_M versus T data for compound **1**·0.5MeOH; the parameters varied were J and g. The data below 10 K was omitted in the fitting because zero-field-splitting and Zeeman effects are likely to have an effect on the susceptibilities in this temperature range. The results of fitting the experimental data are shown as solid lines in Figure 6a, with final parameters of $g = 1.96$, $J_1 = -3.5$ cm^{-1}, $J_2 = -9.3$ cm^{-1}, and $J_3 = -0.2$ cm^{-1}. The temperature-independent paramagnetism (TIP) was held constant at 800×10^{-6} emu mol^{-1}. This set of parameters results in a ground state of $S = {}^3/_2$ for **1**·0.5MeOH, with a very close-lying first excited state ($S = {}^1/_2$) located only 0.8 cm^{-1} above and the second excited state ($S = {}^5/_2$) at 1.2 cm^{-1} above.

For compound **2**·2H$_2$O, $\chi_M T$ slightly decreases from 12.2 emu K mol^{-1} at 300 K to reach a value of 11.7 emu K mol^{-1} at 50 K. Upon cooling, $\chi_M T$ decreases again to 8.6 emu K mol^{-1} at 2.0 K. The value of $\chi_M T$ at 300 K is slightly lower than the calculated spin-only value of 13.4 emu K mol^{-1} for a Mn^{II}Mn$^{III}_3$ compound of noninteracting metal centers with $g = 2.0$, suggesting that weak antiferromagnetic couplings dominate the overall intraunit exchange interactions within the compound. The decreasing $\chi_M T$ at low temperature is likely due to the zero-field-splitting, Zeeman effects and/or intermolecular interactions of the high-spin ground state. Because of the topological complexity of the $(Mn_4)_2$ unit, it is not possible to determine the individual pairwise manganese exchange interactions using the Kambe method.[28] Thus, analysis of the magnetic interactions in **2**·2H$_2$O was simplified into a Mn_4 cluster, which ignores the magnetic interaction between two staggered Mn_4 clusters through a weak interaction of Mn2···O3′ at a distance of 2.736 Å. Considering the C_{3v} symmetry of the Mn_4 cluster in **2**·2H$_2$O, the coupling scheme is shown in Figure 7b. On the basis of the nature of the Mn−Mn distances, a two-J model was used, where J_1 and J_2 characterize the coupling within Mn^{III}−Mn^{III} through μ_3-O^{2-} and oximate bridging and within Mn^{II}−Mn^{III} through $\mu_{1,1}$-N_3^- bridging, respectively. The spin Hamiltonian is given as

$$H = -2J_1(S_1S_2 + S_2S_3 + S_1S_3) - 2J_2(S_1S_4 + S_2S_4 + S_3S_4) \quad (4)$$

The data below 10 K were omitted in the fitting because zero-field-splitting, Zeeman effects and interunit interactions are likely to have an effect on the susceptibilities in this temperature range. The results of fitting the experimental data are shown as solid lines in Figure 7a, with final parameters of $g = 1.91$, $J_1 = 0.7$ cm^{-1}, and $J_2 = -0.6$ cm^{-1}. The TIP was held constant at 800×10^{-6} emu mol^{-1}. This set of parameters

dx.doi.org/10.1021/ic3014333 | Inorg. Chem. 2012, 51, 13171−13180

results in a ground state of $S = {}^{7}/_{2}$ for **2**·2H_2O, with a close-lying first excited state ($S = {}^{9}/_{2}$) located only 5.4 cm^{-1} above and the second excited state ($S = {}^{5}/_{2}$) at 11.3 cm^{-1} above.

The values obtained for the exchange parameters of the two compounds are comparable to those for a similar pathway in other reported compounds. In compound **1**, the intratriangular antiferromagnetic interactions (J_1 and J_2) may result from bridges of μ_3-O^{2-} and the small torsion angles of salicylaldoximate (below 31°). These are consistent with reported compounds that contain a salicylaldoxime-based $[Mn_3O]^{7+}$ triangle.[16c−f,29] The intratriangular interactions in compound **2** (J_1) are ferromagnetic and result from the twisting of Mn−N−O−Mn arrangements with an angle of 43.11°, which is due to the small overlapping of the d_z^2 magnetic orbital for manganese ions[30] and consistent with reported results.[16a,d,29b,31] The small J_1 value in compound **2** may be attributed to the antiferromagnetic interaction between two staggered Mn_4 clusters. The interactions between neighboring Mn^{II} and Mn^{III} ions bridged by end-on N_3^- are antiferromagnetic (J_3 in **1** and J_2 in **2**), which produces the large bridging angles of the azide ions (121.3−127.3° for **1** and 121.7° for **2**).[32]

The S values of the Mn_4 clusters in **1**·0.5MeOH and **2**·2H_2O were confirmed from the variable-temperature and variable-field magnetization (M) measurements in the 2.0−4.0 K and 1−7 T ranges, respectively (Figure S4 and S5 in the Supporting Information). The data were fitted using the program *ANISOFIT*,[33] assuming that only the ground state is populated. However, an acceptable fit could not be obtained using the data collected over the whole field range, which is a common problem because of low-lying excited states if some show an S value greater than that of the ground state. A common solution is to only use data collected with low fields (below 1.0 T).[34] However, it was still not possible to obtain a satisfactory fit assuming that only the ground state is populated in this temperature range. This suggests that both compounds possess particularly low-lying excited states that are populated even at these relatively low temperatures. This is consistent with fitting results for the dc magnetic measurements.

The measurements of the ac magnetic susceptibility were performed on microcrystalline samples for compounds **1**·0.5MeOH and **2**·2H_2O in the temperature range of 1.8−5 K in a zero dc field and a 3.5 G ac field oscillating at frequencies in the range of 100−10000 Hz. The ac susceptibility data for **1**·0.5MeOH are presented in Figure 8, which shows the in-phase ac susceptibility χ_M' (as $\chi_M'T$) versus T (Figure 8, top) and the out-of-phase ac susceptibility χ_M'' versus T (Figure 8, bottom) plots. The sloping $\chi_M'T$ versus T plot is strongly indicative of a population of low-lying excited states because occupation of only the ground state would give an essentially temperature-independent value. At lower temperatures (below 4 K), the in-phase signal decreases and a frequency-dependent χ_M'' signal appears, suggesting slow relaxation of the SMM behavior. However, the peak maxima clearly lie at temperatures below 1.8 K, the operating limit of our instrument. Extrapolation of $\chi_M'T$ data down to 0 K gives ∼1.7 emu K mol^{-1}, indicating an $S = {}^{3}/_{2}$ ground state with $g \sim 1.95$, which is in good agreement with the dc magnetization fits.

The ac magnetic susceptibility data of compound **2**·2H_2O are shown in Figure 9. The $\chi_M'T$ values of **2**·2H_2O are essentially temperature-independent down to ∼4 K, below which they decrease because of slow relaxation. Extrapolate $\chi_M'T$ to a value in the of 9.5 emu K mol^{-1} range at 0 K, suggesting a ground state of $S = {}^{7}/_{2} \pm 1$, which is in good agreement with dc

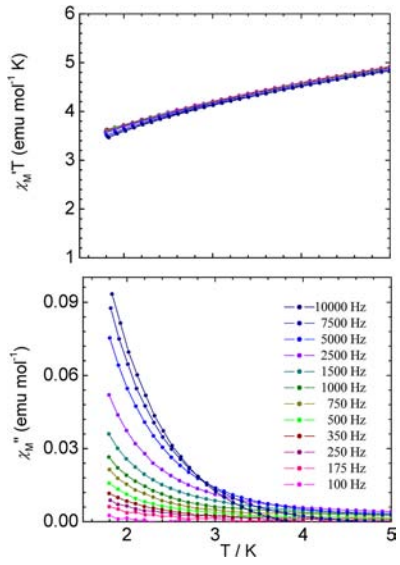

Figure 8. Plots of (top) $\chi_M'T$ and (bottom) χ_M'' versus T for a microcrystalline sample of compound **1**·0.5MeOH in a 3.5 G ac field. The data were collected in an ac field oscillating at the indicated frequency.

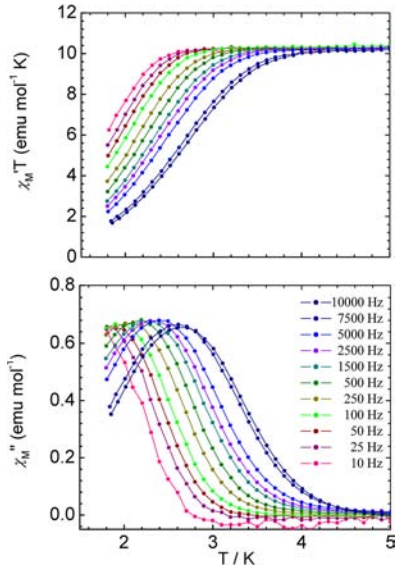

Figure 9. Plots of (top) $\chi_M'T$ and (bottom) χ_M'' versus T for a microcrystalline sample of compound **2**·2H_2O in a 3.5 G ac field. The data were collected in an ac field oscillating at the indicated frequency.

studies.[32b] The out-of-phase χ_M'' signals increased with decreasing temperature; they reached a maximum value at 2.6 K in 10000 Hz and then approached zero, which was frequency dependent. This frequency dependence of the ac signals, which indicates superparamagnetic behavior in compound **2**, is caused by the inability of the compound to relax quickly enough to keep up with the oscillating field at these temperatures. The peak temperatures of χ_M'' can be measured by the parameter $\phi = (\Delta T_p/T_p)/\Delta(\log f) = 0.13$, which is close to the range of normal superparamagnets.[35,36]

In order to confirm the SMM properties, magnetization versus applied dc field data down to 0.04 K were collected on single crystals of **1**·0.5MeOH and **2**·1.5Et_2O using a micro-SQUID apparatus.[37] Magnetization versus dc field scans for single crystals of compounds **1**·0.5MeOH and **2**·1.5Et_2O at

dx.doi.org/10.1021/ic3014333 | *Inorg. Chem.* 2012, 51, 13171−13180

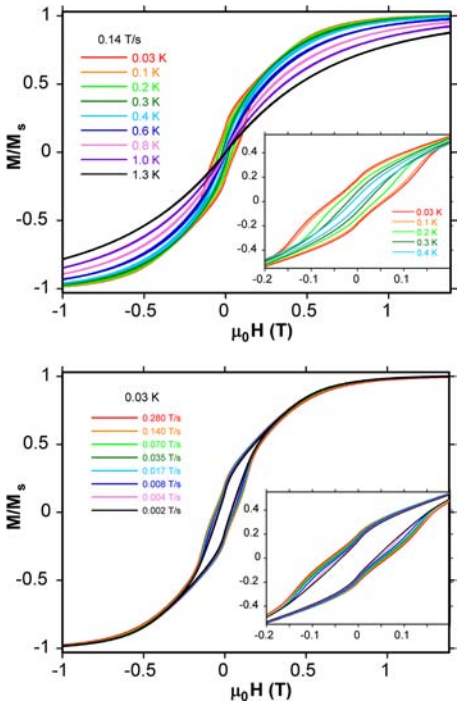

Figure 10. Magnetization hysteresis loops for a single crystal of **1**·0.5MeOH: (top) temperature dependence at a fixed scan rate of 0.14 T/s; (bottom) scan-rate dependence at a fixed temperature of 0.03 K. M is normalized to its saturation value, M_s.

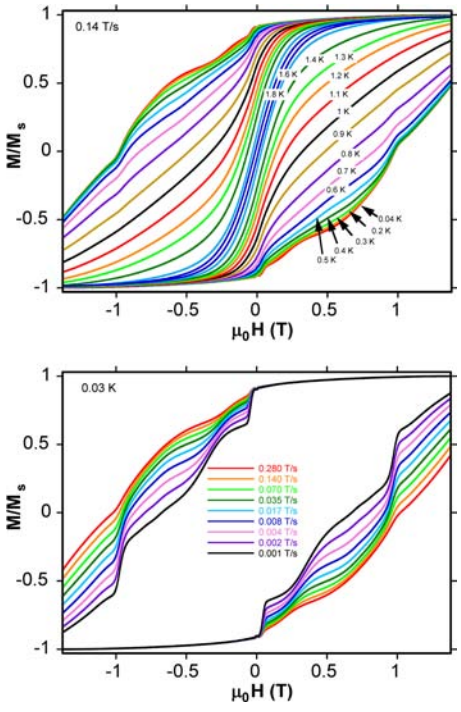

Figure 11. Magnetization hysteresis loops for a single crystal of **2**·1.5Et_2O: (top) temperature dependence at a fixed scan rate of 0.14 T/s; (bottom) scan-rate dependence at a fixed temperature of 0.03 K. M is normalized to its saturation value, M_s.

various temperatures and scan rates are shown in Figures 10−12, respectively. For compound **1**·0.5MeOH, the corresponding magnetization responses are at 0.04−1.3 K and a fixed field sweep rate of 0.14 T/s and magnetization responses at

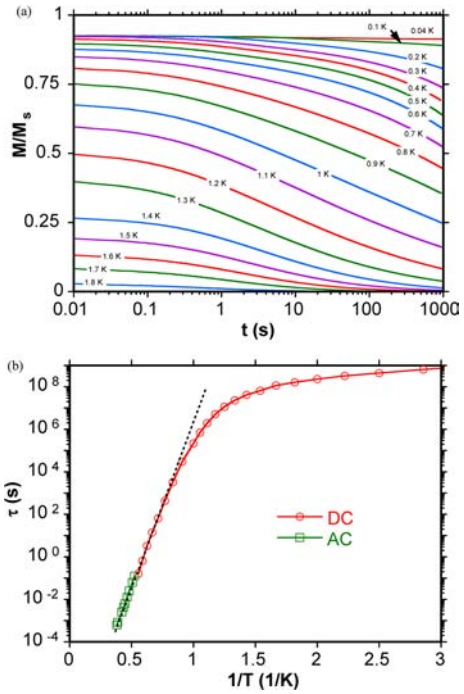

Figure 12. (a) Magnetization decay versus time plots for a single crystal of **2**·1.5Et_2O at the indicated temperatures and (b) relaxation time (τ) versus $1/T$ plot for **2**·1.5Et_2O constructed using dc magnetization decay data. The dashed line is the fit of the thermally activated region to the Arrhenius equation. See the text for the fit parameters.

0.28−0.002 T/s field sweep rates and a constant temperature of 0.03 K. Below 0.4 K, hysteresis loops are observed, whose coercivities increase with increasing field sweep rate and decreasing temperature, indicative of SMM behavior. For compound **2**·1.5Et_2O, the corresponding magnetization responses are at 0.03−1.8 K and a fixed field sweep rate of 0.14 T/s, which shows stepwise magnetization and large coercivities, indicating the occurrence of a quantun tunneling mechanism and significant magnetic anisotropy. Taking into account the crystal structure, we suggest that this large magnetic anisotropy might come from the elongated axes (N1−Mn2···O3) of the six Mn^{III} ions of the two-faced Mn_4 units. Again, the coercivities of the hysteresis loops increase with increasing field sweep rate and decreasing temperature, as expected for the superparamagnet-like behavior of SMMs. Analyzing these hysteresis loops at several field scan rates in more detail, three steps at H = 0, 0.3, and 0.9 T are observed. The steps at H = 0 and 0.9 T are rather sharp, whereas the step at 0.3 T is broad. These steps are probably due to resonant quantum tunneling between ground- and/or excited-state energy levels of the coupled $[Mn_4]_2$ dimer units. In order to determine the effective barrier (U_{eff}) to magnetization relaxation, relaxation rate versus T data at various temperatures down to 0.04 K were obtained from a magnetization decay versus time study (Figure 12). The resulting relaxation rates ($1/\tau$) versus T from ac and dc decay data were used to construct an Arrhenius plot, shown as τ versus $1/T$ in Figure 12, based on the Arrhenius relationship. The fit to the thermally activated region gave $\tau_0 = 4.3 \times 10^{-10}$ s and U_{eff} = 37 K. This effective energy barrier and τ_0 are close to those given for previously reported SMMs.[3−6,11,12,16] Below ∼0.1 K, the relaxation becomes independent of the temperature, consistent with relaxation only via a quantun tunneling mechanism through the anisotropy barrier.

dx.doi.org/10.1021/ic3014333 | Inorg. Chem. 2012, 51, 13171−13180

CONCLUSION

Two new coordination polymers based on mixed-valence tetranuclear manganese $Mn^{III}Mn^{II}$ SMMs, **1**·0.5MeOH and **2**·1.5Et_2O, were self-assembled using the flexible 1,3-di(4-pyridyl)propane (dpp) ligand with coligands of salicylaldoxime and azide. The flexible moiety of dpp modulated **1**·0.5MeOH and **2**·1.5Et_2O, forming a 1D helical chain structure and a 3D framework, respectively. The dc magnetic susceptibility measurements indicate that compounds **1**·0.5MeOH and **2**·1.5Et_2O exhibit intramolecular antiferromagnetic exchange and possess $S = {}^3/_2$ and ${}^7/_2$ ground states, respectively, together with significant magnetic anisotropy, resulting in a small barrier to magnetization relaxation, indicating SMM behavior in both compounds. The results demonstrate that the ligand flexibility of the 1,3-di(4-pyridyl)propane ligands with coligands of salicylaldoxime and azide is a useful motif in the design and synthesis of new multidimensional cluster-based magnetic materials.

ASSOCIATED CONTENT

Supporting Information

TGA results (Figure S1), PXRD data (Figures S2 and S3), reduced magnetization data (Figures S4 and S5), and crystallographic files in CIF format. This material is available free of charge via the Internet at http://pubs.acs.org.

AUTHOR INFORMATION

Corresponding Author

*E-mail: hltsai@mail.ncku.edu.tw (H.-L.T.), ciyang@thu.edu.tw (C.-I.Y.). Tel.: +886 6 275 7575 ext. 65349. Fax: +886 6 274 0552.

Notes

The authors declare no competing financial interest.

ACKNOWLEDGMENTS

The magnetic measurements were obtained from SQUID (MPMS XL-7) in NSYSU. The authors thank the National Science Council of Taiwan (Grant NSC-99-2113-M-006-003-MY3) and the ERC Advanced Grant MolNanoSpin 226558 for financial support.

REFERENCES

(1) (a) Ferreira, K. N.; Iverson, T. M.; Maghlaoui, K.; Barber, J.; Iwata, S. *Science* **2004**, *303*, 1831. (b) Carrell, T. G.; Tyryshkin, A. M.; Dismukes, G. C. *J. Biol. Inorg. Chem.* **2002**, *7*, 2. (c) Cinco, R. M.; Rompel, A.; Visser, H.; Aromí, G.; Christou, G.; Sauer, K.; Klein, M. P.; Yachandra, V. K. *Inorg. Chem.* **1999**, *38*, 5988. (d) Yachandra, V. K.; Sauer, K.; Klein, M. P. *Chem. Rev.* **1996**, *96*, 2927.

(2) Pecoraro, V. L. *Manganese Redox Enzymes*; VCH: New York, 1992.

(3) (a) Christou, G.; Gatteschi, D.; Hendrickson, D. N.; Sessoli, R. *MRS Bull.* **2000**, *25*, 66. (b) Sessoli, R.; Tsai, H.-L.; Schake, A. R.; Wang, S.; Vincent, J. B.; Folting, K.; Gatteschi, D.; Christou, G.; Hendrickson, D. N. *J. Am. Chem. Soc.* **1993**, *115*, 1804. (c) Caneschi, A.; Gatteschi, D.; Sessoli, R.; Barra, A. L.; Brunel, L. C.; Guillot, M. *J. Am. Chem. Soc.* **1991**, *113*, 5873. (d) Nakano, M.; Oshio, H. *Chem. Soc. Rev.* **2011**, *40*, 3239.

(4) (a) Sessoli, R.; Gatteschi, D.; Caneschi, A.; Novak, M. A. *Nature* **1993**, *365*, 141. (b) Gatteschi, D.; Sessoli, R.; Cornia, A. *Chem. Commun.* **2000**, 725. (c) Sun, Z. M.; Grant, C. M.; Castro, S. L.; Hendrickson, D. N.; Christou, G. *Chem. Commun.* **1998**, 721. (d) Yang, E. C.; Hendrickson, D. N.; Wernsdorfer, W.; Nakano, M.; Zakharov, L. N.; Sommer, R. D.; Rheingold, A. L.; Ledezma-Gairaud, M.; Christou, G. *J. Appl. Phys.* **2002**, *91*, 7382.

(5) (a) Andres, H.; Basler, R.; Blake, A. J.; Cadiou, C.; Chaboussant, G.; Grant, C. M.; Güdel, H. U.; Murrie, M.; Parsons, S.; Paulsen, C.; Semadini, F.; Villar, V.; Wernsdorfer, W.; Winpenny, R. E. P. *Chem.—Eur. J.* **2002**, *8*, 4867. (b) Murugesu, M.; Mishra, A.; Wernsdorfer, W.; Abboud, K. A.; Christou, G. *Polyhedron* **2006**, *25*, 613. (c) Yang, C.-I.; Wernsdorfer, W.; Tsai, Y.-J.; Chung, G.; Kuo, T.-S.; Lee, G.-H.; Shieh, M.; Tsai, H.-L. *Inorg. Chem.* **2008**, *47*, 1925.

(6) (a) Christou, G. *Polyhedron* **2005**, *24*, 2065. (b) Gatteschi, D.; Sessoli, R.; Villain, J. *Molecular Nanomagnets*; Oxford University Press: New York, 2006. (c) Aromí, G.; Brechin, E. K. *Struct. Bonding (Berlin)* **2006**, *122*, 1 and references cited therein.

(7) (a) Coulon, C.; Miyasaka, H.; Clérac, R. *Struct. Bonding (Berlin)* **2006**, *122*, 163. (b) Miyasaka, H.; Julve, M.; Yamashita, M.; Clérac, R. *Inorg. Chem.* **2009**, *48*, 3420 and references cited therein.

(8) (a) Clérac, R.; Miyasaka, H.; Yamashita, M.; Coulon, C. *J. Am. Chem. Soc.* **2002**, *124*, 12837. (b) Caneschi, A.; Gatteschi, D.; Lalioti, N.; Sangregorio, C.; Sessoli, R.; Venturi, G.; Vindigni, A.; Rettori, A.; Pini, M. G.; Novak, M. A. *Angew. Chem., Int. Ed.* **2001**, *40*, 1760.

(9) (a) Lecren, L.; Roubeau, O.; Coulon, C.; Li, Y.-G.; Le Goff, X. F.; Wernsdorfer, W.; Miyasaka, H.; Clérac, R. *J. Am. Chem. Soc.* **2005**, *127*, 17353. (b) Yoo, J.; Wernsdorfer, W.; Yang, E.-C.; Nakano, M.; Rheingold, A. L.; Hendrickson, D. N. *Inorg. Chem.* **2005**, *44*, 3377. (c) Glauber, R. J. *J. Math. Phys.* **1963**, *4*, 294. (d) Bogani, L.; Caneschi, A.; Fedi, M.; Gatteschi, D.; Massi, M.; Novak, M. A.; Pini, M. G.; Rettori, A.; Sessoli, R.; Vindigni, A. *Phys. Rev. Lett.* **2004**, *92*, 207204. (e) Przybylak, S. W.; Tuna, F.; Teat, S. J.; Winpenny, R. E. P. *Chem. Commun.* **2008**, 1983. (f) Palii, A. V.; Reu, O. S.; Ostrovsky, S. M.; Klokishner, S. I.; Tsukerblat, B. S.; Sun, Z.-M.; Mao, J.-G.; Prosvirin, A. V.; Zhao, H.-H.; Dunbar, K. R. *J. Am. Chem. Soc.* **2008**, *130*, 14729. (g) Harris, T. D.; Bennett, M. V.; Clérac, R.; Long, J. R. *J. Am. Chem. Soc.* **2010**, *132*, 3980.

(10) (a) Yoo, J.; Yamaguchi, A.; Nakano, M.; Krzystek, J.; Streib, W. E.; Brunel, L.-C.; Ishimoto, H.; Christou, G.; Hendrickson, D. N. *Inorg. Chem.* **2001**, *40*, 4604. (b) Brechin, E. K.; Boskovic, C.; Wernsdorfer, W.; Yoo, J.; Yamaguchi, A.; Sañudo, E. C.; Concolino, T. R.; Rheingold, A. L.; Ishimoto, H.; Hendrickson, D. N.; Christou, G. *J. Am. Chem. Soc.* **2002**, *124*, 9710. (c) Boskovic, C.; Brechin, E.; Streib, W. E.; Folting, K.; Bollinger, J. C.; Hendrickson, D. N.; Christou, G. *J. Am. Chem. Soc.* **2002**, *124*, 3725.

(11) (a) Tasiopoulos, A. J.; Wernsdorfer, W.; Moulton, B.; Zaworotko, M. J.; Christou, G. *J. Am. Chem. Soc.* **2003**, *125*, 15274. (b) Miyasaka, H.; Madanbashi, T.; Sugimoto, K.; Nakazawa, Y.; Wernsdorfer, W.; Sugiura, K.; Yamashita, M.; Coulon, C.; Clérac, R. *Chem.—Eur. J.* **2006**, *12*, 7028. (c) Bernot, K.; Luzon, J.; Sessoli, R.; Vindigni, A.; Thion, J.; Richeter, S.; Leclercq, D.; Larionova, J.; van der Lee, A. *J. Am. Chem. Soc.* **2008**, *130*, 1619. (d) Zhang, Y.; Wang, X.-T.; Zhang, X.-M.; Liu, T.-F.; Xu, W.-G.; Gao, S. *Inorg. Chem.* **2010**, *49*, 5868. (e) Bogani, L.; Vindigni, A.; Sessoli, R.; Gatteschi, D. *J. Mater. Chem.* **2008**, *18*, 4750.

(12) (a) Chakov, N. E.; Wernsdorfer, W.; Abboud, K. A.; Christou, G. *Inorg. Chem.* **2004**, *43*, 5919. (b) Stamatatos, T. C.; Abboud, K. A.; Wernsdorfer, W.; Christou, G. *Inorg. Chem.* **2009**, *48*, 807. (c) Escuer, A.; Vlahopoulou, G.; Mautner, F. A. *Inorg. Chem.* **2011**, *50*, 2717. (d) Sun, H.-L.; Wang, Z.-M.; Gao, S. *Coord. Chem. Rev.* **2010**, *254*, 1081.

(13) (a) Roubeau, O.; Clérac, R. *Eur. J. Inorg. Chem.* **2008**, 4325 and references cited therein. (b) Miyasaka, H.; Nakata, K.; Lecren, L.; Coulon, C.; Nakazawa, Y.; Fujisaki, T.; Sugiura, K.; Yamashita, M.; Clérac, R. *J. Am. Chem. Soc.* **2006**, *128*, 3770. (c) Burzurí, E.; Campo, J.; Falvello, L. R.; Forcén-Vázquez, E.; Luis, F.; Mayoral, I.; Palacio, F.; de Pipaón, C. S.; Tomás, M. *Chem.—Eur. J.* **2011**, *17*, 2818.

(14) (a) Moushi, E. E.; Stamatatos, T. C.; Wernsdorfer, W.; Nastopoulos, V.; Christou, G.; Tasiopoulos, A. J. *Angew. Chem., Int. Ed.* **2006**, *45*, 7722. (b) Miyasaka, H.; Nakata, K.; Sugiura, K.; Yamashita, M.; Clérac, R. *Angew. Chem., Int. Ed.* **2004**, *43*, 707. (c) Stamatatos, T. C.; Abboud, K. A.; Christou, G. *J. Cluster Sci.* **2010**, *21*, 485.

(15) (a) Moushi, E. E.; Stamatatos, T. C.; Nastopoulos, V.; Christou, G.; Tasiopoulos, A. J. *Polyhedron* **2009**, *28*, 1814. (b) Nguyen, T. N.;

Wernsdorfer, W.; Abboud, K. A.; Christou, G. *J. Am. Chem. Soc.* **2011**, *133*, 20688.
(16) (a) Yang, C.-I.; Wernsdorfer, W.; Lee, G.-H.; Tsai, H.-L. *J. Am. Chem. Soc.* **2007**, *129*, 456. (b) Yang, C.-I.; Wernsdorfer, W.; Cheng, K.-H.; Nakano, M.; Lee, G.-H.; Tsia, H.-L. *Inorg. Chem.* **2008**, *47*, 10184. (c) Milios, C. J.; Wood, P. A.; Parsons, S.; Foguet-Albiol, D.; Lampropoulos, C.; Christou, G.; Perlepes, S. P.; Brechin, E. K. *Inorg. Chim. Acta* **2007**, *360*, 3932. (d) Milios, C. J.; Vinslava, A.; Whittaker, A. G.; Parsons, S.; Wernsdorfer, W.; Christou, G.; Perlepes, S. P.; Brechin., E. K. *Inorg. Chem.* **2006**, *45*, 5272. (e) Lampropoulos, C.; Abboud, K. A.; Stamatatos, T. C.; Christou, G. *Inorg. Chem.* **2009**, *48*, 813. (f) Cano, J.; Cauchy, T.; Ruiz, E.; Milios, C. J.; Stoumpos, C. C.; Stamatatos, T. C.; Perlepes, S. P.; Christou, G.; Brechin, E. K. *Dalton Trans.* **2008**, 234. (g) Stamatatos, T. C.; Abboud, K. A.; Wernsdorfer, W.; Christou, G. *Polyhedron* **2007**, *26*, 2095. (h) Yang, C.-I.; Cheng, K.-H.; Nakano, M.; Lee, G.-H.; Tsai, H.-L. *Polyhedron* **2009**, *28*, 1842. (i) Liu, M.-H.; Yang, C.-I.; Lee, G.-H.; Tsai, H.-L. *Inorg. Chem. Commun.* **2011**, *14*, 1136.
(17) (a) Yang, C.-I.; Tsai, Y.-J.; Hung, S.-P.; Tsai, H.-L.; Nakano, M. *Chem. Commun.* **2010**, *46*, 5716. (b) Jones, L. F.; Prescimone, A.; Evangelisti, M.; Brechin, E. K. *Chem. Commun.* **2009**, 2023.
(18) (a) Murugesu, M.; Habrych, M.; Wernsdorfer, W.; Abboud, K. A.; Christou, G. *J. Am. Chem. Soc.* **2004**, *126*, 4766. (b) Ako, A. M.; Hewitt, I. J.; Mereacre, V.; Clérac, R.; Wernsdorfer, W.; Anson, C. E.; Powell, A. K. *Angew. Chem., Int. Ed.* **2006**, *45*, 4926. (c) Stamatatos, T. C.; Abboud, K. A.; Wernsdorfer, W.; Christou, G. *Angew. Chem., Int. Ed.* **2007**, *46*, 884. (e) Brockman, J. T.; Stamatatos, T. C.; Wernsdorfer, W.; Abboud, K. A.; Christou, G. *Inorg. Chem.* **2007**, *46*, 9160. (f) Stamatatos, T. C.; Christou, G. *Inorg. Chem.* **2009**, *48*, 3308 and references cited therein.
(19) (a) Xu, H. B.; Wang, B. W.; Pan, F.; Wang, Z. M.; Gao, S. *Angew. Chem., Int. Ed.* **2007**, *46*, 7388. (b) Feng, P. L.; Hendrickson, D. N. *Inorg. Chem.* **2010**, *49*, 6393. (c) Yang, C.-I.; Hung, S. P.; Lee, G.-H.; Nakano, M.; Tsai, H.-L. *Inorg. Chem.* **2010**, *49*, 7617.
(20) Dunsten, W. R.; Henry, T. A. *J. Chem. Soc.* **1899**, *75*, 66.
(21) Sheldrick, G. M. *SHELXL-97*; University of Gottingen: Gottingen, Germany, 1997.
(22) Boudreaux, E. A.; Mulay, L. N. *Theory and Application of Molecular Paramagnetism*; John Wiley & Sons: New York, 1976; p 491.
(23) (a) Inglis, R.; White, F.; Piligkos, S.; Wernsdorfer, W.; Brechin, E. K.; Papaefstathiou, G. S. *Chem. Commun.* **2011**, *47*, 3090. (b) Mason, K.; Gass, I. A.; Parsons, S.; Collins, A.; White, F. J.; Slawin, A. M. Z.; Brechin, E. K.; Tasker, P. A. *Dalton Trans.* **2010**, *39*, 2727. (c) Mason, K.; Gass, I. A.; White, F. J.; Papaefstathiou, G. S.; Brechin, E. K.; Tasker, P. A. *Dalton Trans.* **2011**, *40*, 2875. (d) Li, B.-W.; Zhou, Y.-L.; Chen, Q.; Zeng, M.-H. *Polyhedron* **2010**, *29*, 148.
(24) (a) Lalia-Kantouri, M.; Hatzidimitriou, A.; Uddin, M. *Polyhedron* **1999**, *18*, 3441. (b) Lalia-Kantouri, M.; Uddin, M.; Hadjikostas, C. C.; Papanikolas, H.; Palios, G.; Anagnostis, S.; Anesti, V. *Z. Anorg. Allg. Chem.* **1997**, *623*, 1983. (c) Lalia-Kantouri, M.; Hartophylles, M.; Jannakoudakis, P. D.; Voutsas, G. P. *Z. Anorg. Allg. Chem.* **1995**, *621*, 645. (d) Voutsas, G. P.; Keramidas, K. G.; Lalia-Kantouri, M. *Polyhedron* **1996**, *15*, 147.
(25) (a) Thorpe, J. M.; Beddoes, R. L.; Collison, D.; Garner, C. D.; Helliwell, M.; Holmes, J. M.; Tasker, P. A. *Angew. Chem., Int. Ed.* **1999**, *89*, 1119. (b) Milios, C. J.; Raptopoulou, C. P.; Terzis, A.; Lloret, F.; Vicente, R.; Perlepes, S. P.; Escuer, A. *Angew. Chem., Int. Ed.* **2004**, *43*, 210. (c) Raptopoulou, C. P.; Boudalis, A. K.; Sanakis, Y.; Psycharis, V.; Clemente-Juan, J. M.; Fardis, M.; Diamantopoulos, G.; Papavassiliou, G. *Inorg. Chem.* **2006**, *45*, 2317.
(26) (a) Liu, W.; Thorp, H. H. *Inorg. Chem.* **1993**, *32*, 4102. (b) Brown, I. D.; Altermatt, D. *Acta Crystallogr., Sect. B* **1985**, *41*, 244.
(27) Addison, A. W.; Rao, T. N.; Reedijk, J.; Rijn, J. V.; Verschoor, G. C. *J. Chem. Soc., Dalton Trans.* **1984**, 1349.
(28) Kambe, K. J. *Phys. Soc. Jpn.* **1950**, *5*, 48.
(29) (a) Inglis, R.; Katsenis, A. D.; Collins, A.; White, F.; Milios, C. J.; Papaefstathiou, G. S.; Brechin, E. K. *CrystEngComm* **2010**, *12*, 2064. (b) Stoumpos, C. C.; Inglis, R.; Karotsis, G.; Jones, L. F.; Collins, A.; Parsons, S.; Milios, C. J.; Papaefstathiou, G. S.; Brechin, E. K. *Cryst. Growth Des.* **2009**, *9*, 24. (c) Inglis, R.; Taylor, S. M.; Jones, L. F.; Papaefstathiou, G. S.; Perlepes, S. P.; Datta, S.; Hill, S.; Wernsdorfer, W.; Brechin, E. K. *Dalton Trans.* **2009**, 9157. (d) Feng, P. L.; Koo, C.; Henderson, J. J.; Nakano, M.; Hill, S.; del Barco, E.; Hendrickson, D. N. *Inorg. Chem.* **2008**, *47*, 8610. (e) Kozoni, C.; Manolopoulou, E.; Siczek, M.; Lis, T.; Brechin, E. K.; Milios, C. J. *Dalton Trans.* **2010**, *39*, 7943.
(30) (a) Cremades, E.; Cano, J.; Ruiz, E.; Rajaraman, G.; Milios, C. J.; Brechin, E. K. *Inorg. Chem.* **2009**, *48*, 8012. (b) Atanasov, M.; Delley, B.; Neese, F.; Tregenna-Piggott, P. L.; Sigrist, M. *Inorg. Chem.* **2011**, *50*, 2112.
(31) (a) Inglis, R.; Jones, L. F.; Karotsis, G.; Collins, A.; Parsons, S.; Perlepes, S. P.; Wernsdorfer, W.; Brechin, E. K. *Chem. Commun.* **2008**, 5924. (b) Inglis, R.; Jones, L. F.; Mason, K.; Collins, A.; Moggach, S. A.; Parsons, S.; Perlepes, S. P.; Wernsdorfer, W.; Brechin, E. K. *Chem.—Eur. J.* **2008**, *14*, 9117. (c) Milios, C. J.; Prescimone, A.; Mishra, A.; Parsons, S.; Wernsdorfer, W.; Christou, G.; Perlepes, S. P.; Brechin., E. K. *Chem. Commun.* **2007**, 153. (d) Milios, C. J.; Vinslava, A.; Wood, P. A.; Parsons, S.; Wernsdorfer, W.; Christou, G.; Perlepes, S. P.; Brechin., E. K. *J. Am. Chem. Soc.* **2007**, *129*, 8. (e) Milios, C. J.; Inglis, R.; Bagai, R.; Wernsdorfer, W.; Collins, A.; Moggach, S.; Parsons, S.; Perlepes, S. P.; Christou, G.; Brechin, E. K. *Chem. Commun.* **2007**, 3476.
(32) (a) Milios, C. J.; Inglis, R.; Vinslava, A.; Prescimone, A.; Parsons, S.; Perlepes, S. P.; Christou, G.; Brechin, E. K. *Chem. Commun.* **2007**, 2738. (b) Milios, C. J.; Inglis, R.; Jones, L. F.; Prescimone, A.; Parsons, S.; Wernsdorfer, W.; Brechin, E. K. *Dalton Trans.* **2009**, 2812.
(33) Shores, M. P.; Sokol, J. J.; Long, J. R. *J. Am. Chem. Soc.* **2002**, *124*, 2279.
(34) (a) Brechin, E. K.; Sanudo, E. C.; Wernsdorfer, W.; Boskovic, C.; Yoo, J.; Hendrickson, D. N.; Yamaguchi, A.; Ishimoto, H.; Concolino, T. E.; Rheingold, A. L.; Christou, G. *Inorg. Chem.* **2005**, *44*, 502. (b) Stamatatos, T. C.; Luisi, B. S.; Moulton, B.; Christou, G. *Inorg. Chem.* **2008**, *47*, 1134. (c) Sañudo, E. C.; Wernsdorfer, W.; Abboud, K. A.; Christou, G. *Inorg. Chem.* **2004**, *43*, 4137. (d) Tasiopoulos, A. J.; Wernsdorfer, W.; Abboud, K. A.; Christou, G. *Inorg. Chem.* **2005**, *44*, 6324. (e) Murugesu, M.; Raftery, J.; Wernsdorfer, W.; Christou, G.; Brechin, E. K. *Inorg. Chem.* **2004**, *43*, 4203.
(35) (a) Ferbinteanu, M.; Miyasaka, H.; Wernsdorfer, W.; Nakata, K.; Sugiura, K.; Yamashita, M.; Coulon, C.; Clérac, R. *J. Am. Chem. Soc.* **2005**, *127*, 3090. (b) Bernot, K.; Bogani, L.; Caneschi, A.; Gatteschi, D.; Sessoli, R. *J. Am. Chem. Soc.* **2006**, *128*, 7947.
(36) Mydosh, J. A. *Spin Glasses: An Experimental Introduction*; Taylor & Francis: London, 1993.
(37) Wernsdorfer, W. *Adv. Chem. Phys.* **2001**, *118*, 99.